11th Baltic Sea Geotechnical Conference
GEOTECHNICS IN MARITIME ENGINEERING
Gdansk, Poland
15–18 September 2008

Load Transfer Mechanism of Geogrids in Pile Supported Embankments

Hans-Georg Kempfert
Jan Lüking
Berhane Gebreselassie
University of Kassel, Institute of Geotechnics and Geohydraulics, Germany

ABSTRACT
Geosynthetic reinforced and pile supported embankments (GPE) are often used to transfer traffic loads into a bearing layer through a soft soil layer. Usually uniaxial or biaxial geogrids are used as reinforcement in embankments. The effect of pile configuration on mechanical behaviour of the load transfer from the geogrids to the piles have not been yet fully investigated. For this purpose large scale model tests using different pile configurations (rectangular and triangular grid system) and numerical calculations had been conducted. The result of the tests show that the load transfer in a rectangular grid system can be confirmed. Nevertheless, a transference of this model representation to a triangular grid system is problematic. For the arrangement of the pile-like elements in a triangular grid system a new model representation is derived from numerical calculations and a modified analysis is suggested.

1 INTRODUCTION

With the help of geosynthetic reinforced and pile supported embankments, known as GPE, static and dynamic transport loads can be transferred directly to the bearing layer and thus relief the soft underground. The GPE system is successfully used in the construction industry since beginning of the 1990 (see Kempfert and Stadel 1995). The main application area of the GPE system is railway and road embankments on soft to very soft underground.

In the last years, many researchers have dedicated themselves to this topic with different type of model concept. A summarised overview of the different models can be found in Heitz (2006).

The load transfer mechanism of a GPE system is based on soil arching developed in the embankment as shown in Fig. 1. Part of the load is carried directly by the pile-like elements due to the soil arching, part of it by the geosynthetic, often geogrids, and the rest by the soil reaction in the soft layer. Thus, the soft

underground is relieve and as a result less settlement is expected.

The current method of design of a GPE system is given for example in EBGEO (2008) (German recommendations geosynthetic reinforcements), which is developed based on the arching model by Zaeske (2001) (see also Zaeske and Kempfert, 2002). However, this design method does not yet include all factors affecting the GPE system. Rather it partly lies on the safe side. One of these factors is the load transfer mechanism in the geogrids, especially by triangular grid arrangement of the pile-like elements.

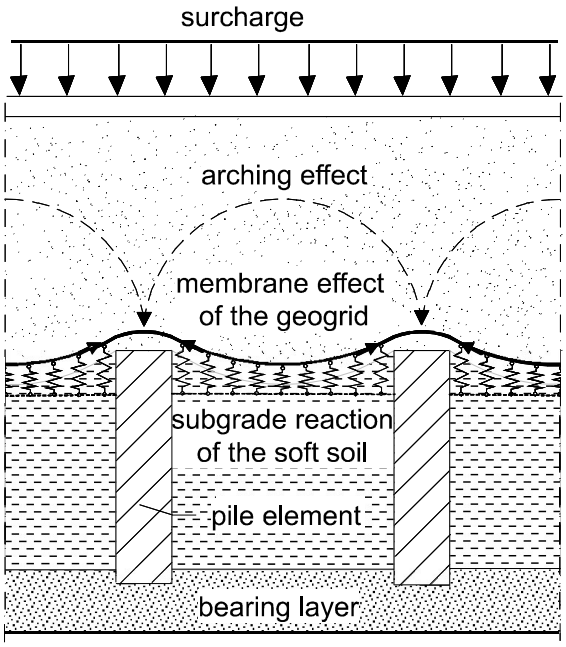

Fig. 1. Load transfer mechanism of a GPE System

For further investigation of the load transfer mechanism of the GPE system, in particular the mechanism in the case of rectangular and triangular pile arrangements, a series of model tests and numerical studies had been conducted at the department of geotechnics, University of Kassel. The results sorted out according to the grid arrangement of the pile-like elements are presented in the following.

2 RECTANGULAR GRID SYSTEM

2.1 Model Test

The goal of the model tests was the investigation of the load transfer mechanism of the geogrids depending on the type of grid used for the arrangement of the pile-like elements.

The model tests were conducted using the model box developed by Zaeske (2001) and further modified by Heitz (2006). The model represents a section in the central part of the GPE system without the slopes at a scale of 1:3. As shown in Fig. 2 the model consists of four pile elements.

A series of test was conducted with which two different types of geogrids and pile arrangements have been investigated. In the following only those tests that are numerically analysed afterwards are presented. Detail description of the tests as well as the material used can be found in Lueking et al. (2008).

As shown in Fig. 2, up to three pressure transducers were installed at different locations of the sand layer. Strain gauges had been applied on the surface of the geogrids strips to measure the stain and thus to estimate the tensile stress.

The loading was followed incrementally in 15 load steps each with 8.3 kN/m^2 and for duration of 30 min.

Fig. 3 shows the strain in the geogrids for selected strain gauges in the case of rectangular grid. It can be seen from Fig. 3 that the largest strains are recorded in the shortest direction between the piles (strain gauges 3, 11 and 12). On the other hand a very small strain was measured in the middle (e.g. strain gauges 1 and 7).

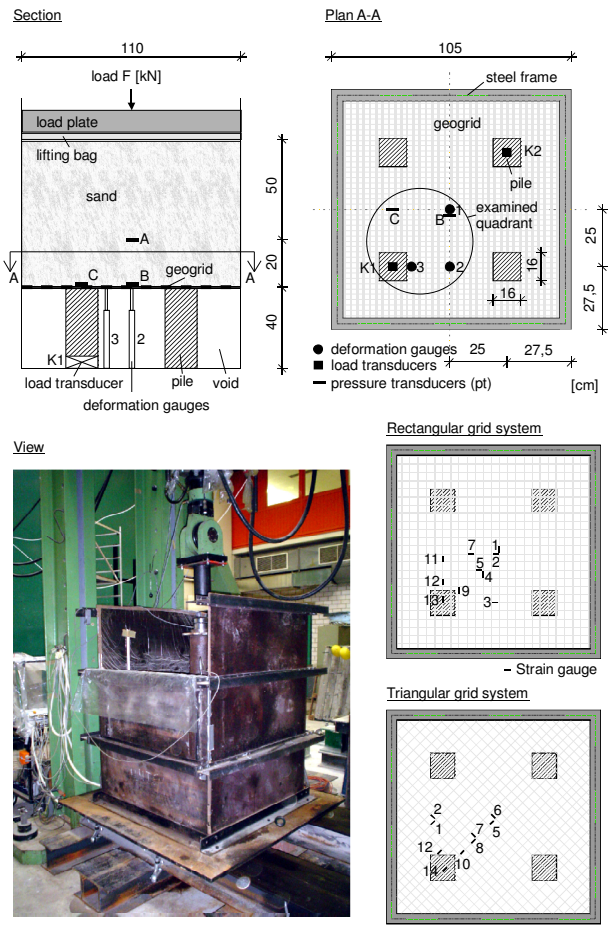

Fig. 2. Model test arrangement

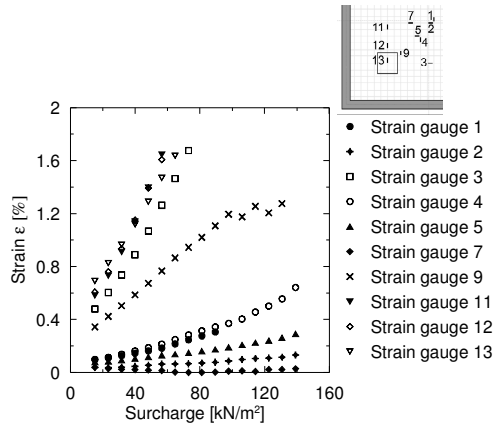

Fig. 3. Strains in geogrids (rectangular grid)

2.2 Numerical Analysis

The numerical analysis was conducted using the program RSTAB Version 5. The geogrid was simulated as linear-elastic wire. The wires are connected at the nodes with hinges. The soil pressure was applied on the nodes as concentrated loads. The numerical models used for rectangular and triangular grid system is shown in Fig. 4. Such kind of simplified approach is already reported by Heitz (2006). The objective of the numerical analysis is the determination of the distribution of vertical stresses on the surface of the geogrids and hence the study of the soil arching in the embankment.

From the measured pressures directly above the geogrids, concentrated nodal forces F were derived for the numeric computations, in which the soil pressure was assumed constant within the influence area $a \cdot a$ (see Fig. 4).

In areas where no soil pressure had been measured in the model test, then nodal forces had been optimised iteratively until an agreement reached between the measured and calculated strain in the geogrids.

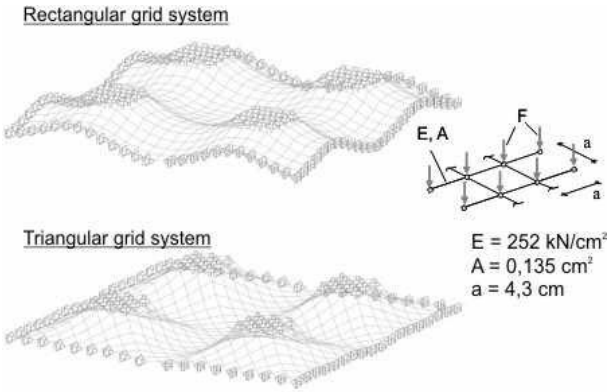

Fig. 4. Numerical models for rectangular and triangular grid systems

A comparison of the measured and calculated strains in the geogrids is indicated in Fig. 5 for the case of rectangular grid system. Whereas Fig. 6 and 7 show the comparison of the measured and computed pile reaction and deflection of the geogrids respectively.

The optimised nodal forces were then converted to uniformly distributed soil pressure within the influence area in order to estimate

the possible pressure distribution in the model test at the top surface of the geogrids (Fig. 8).

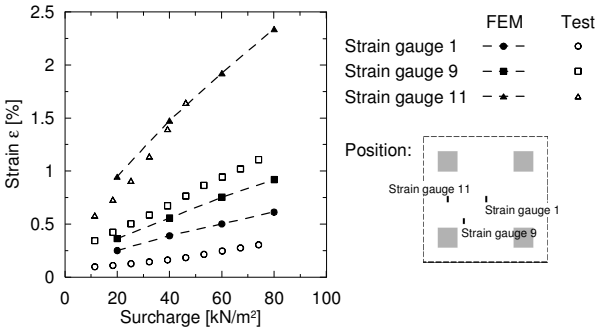

Fig. 5. Comparison of measured and calculated strains (rectangular grid)

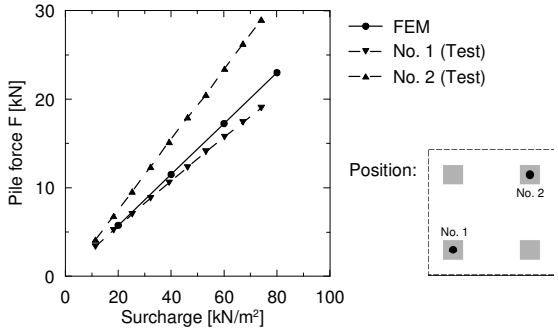

Fig. 6. Comparison of the measured and calculated pile reaction (rectangular grid)

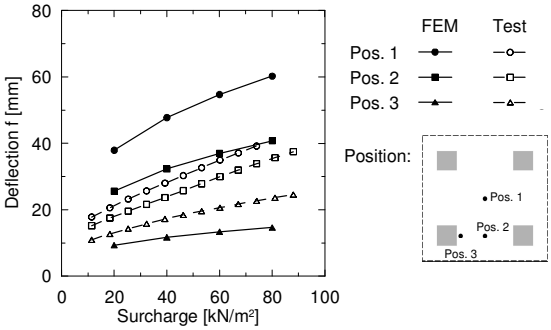

Fig. 7. Comparison of the measured and calculated deflection of the geogrids (rectangular grid)

In Fig. 8 a higher stress concentration can be observed at pile tops. Compared to the middle area, a higher pressure was calculated in zone of the shortest distance between the piles.

The calculated vertical soil pressures at the top surface of the geogrids are compared with values measured by Zaeske (2001) as shown in Fig. 9.

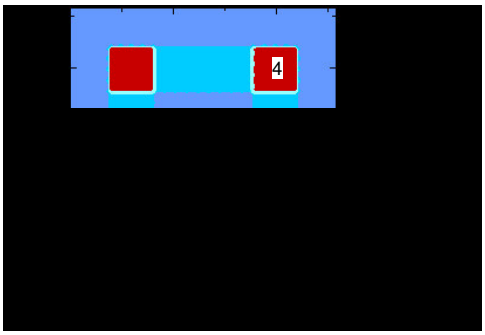

Fig. 8. Soil pressure distribution on the top surface of the geogrids based on numerical calculation (rectangular grid)

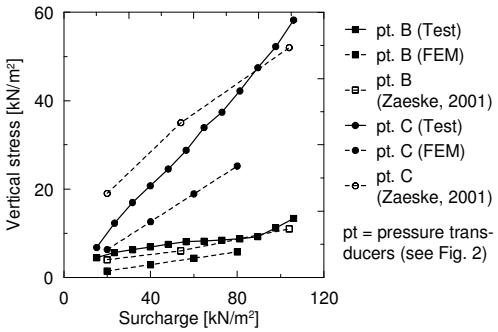

Fig. 9. Comparison of the measured and calculated soil pressures

The higher stress concentration on the pile top results from the soil arching as it serves as a base for the arch. The relatively higher vertical soil pressure along the shortest distance between the piles also shows there exist additional soil arching that uses these areas as a linear base. This is a confirmation to the concept of soil arching developed by Heitz (2006) as shown in Fig. 10.

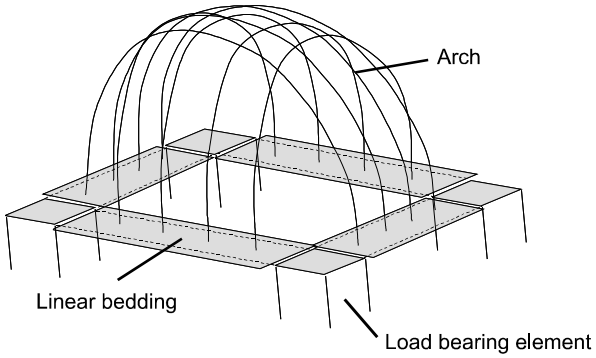

Fig. 10. Development of soil arching in case of rectangular grid after Heitz (2006)

3 TRIANGULAR GRID SYSTEM

3.1 Model Test

In order to simulate the triangular grid arrangement of the pile like elements in the same model box as in Section 2.1, the geogrids was fixed to the steel frame at angle of 45°. Otherwise the performance of the test remains the same as in the case of rectangular grid system (Section 2.1).

Fig. 11 shows the strain in geogrids from selective strain gauges. It can be seen from the Fig. 11 that the strain in triangular grid system shows quite another trend. The largest strains were recorded by strain gauges 5, 8 and 14, which are located in the diagonal direction between the piles. Whereas those strain gauges, which are arranged in the direction of the shortest distance between the piles (e.g. strain gauges 1 and 2), had been subjected to less strain.

3.2 Numerical Analysis

Since no soil pressure had been measured in these series of tests, the concentrated nodal forces are varied incrementally till an agreement had been reached between the measured and calculated strains in the geogrids strips. See also Section 2.2. The results are shown in Fig. 12.

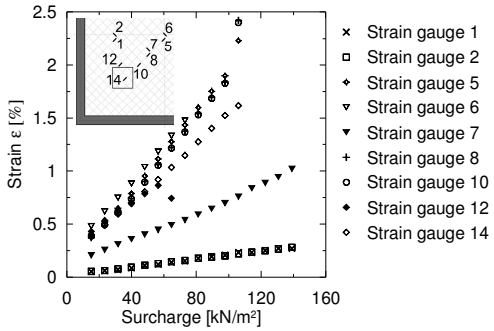

Fig. 11. Strains in geogrids (triangular grid)

Similar to the rectangular grid system, the soil pressure and its distribution on the top surface of the geogrids was estimated based on the calibrated nodal forces and the influence are as shown in Fig. 13. It can be observed that the stress concentration on the top of the pile is higher compared to rectangular grid system, which indicates a stronger soil arching. The soil pressures on the geogrids are relatively uniformly distributed and are smaller compared to rectangular grid. However, there exists a higher local stress concentration in the middle of the geogrids (Fig. 13).

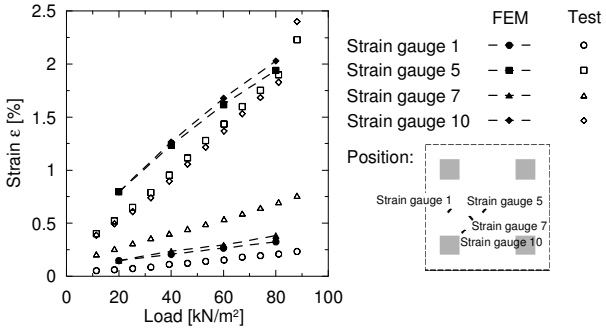

Fig. 12. Comparison of measured and calculated strains (triangular grid)

Fig. 14 and 15 show the measured and calculated pile reaction and deflection of the geogrids.

Because of the different vertical soil pressure distribution compared to the rectangular grid system, it is assumed that the form of the soil arching is also different. The smaller soil pressure in the direction of the shortest dis-

tance between the piles indicates that no linear base support is available for the soil arching as in the case of the rectangular grid system. On the other hand, the high local stress concentration in the middle shows a point base support for the soil arching at this location. However, this hypothesis has to be verified by further study.

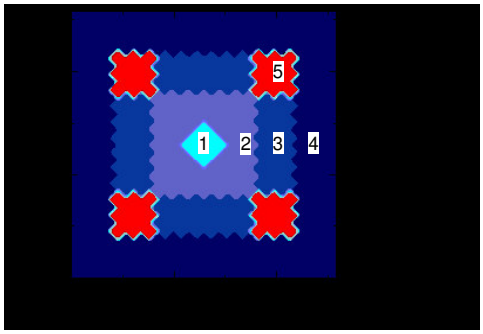

Fig. 13. Soil pressure distribution on the top surface of the geogrids based on numerical calculation (triangular grid)

The different form of the base support results in a reduced span length of the arch, and hence a stronger soil arching may be possible. The higher stress concentration on the top of the piles compared to rectangular grid system may support this hypothesis (compare Fig. 13 and 7). Fig. 16 shows the possible form of soil arching in the case of a triangular grid system.

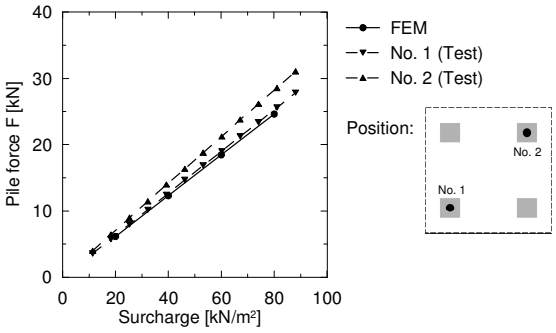

Fig. 14. Comparison of the measured and calculated pile reaction (triangular grid)

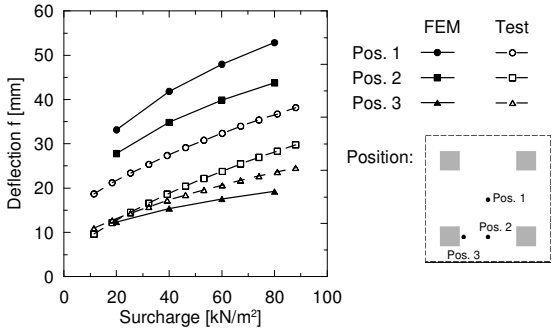

Fig. 15. Comparison of the measured and calculated deflection of the geogrids (triangular grid)

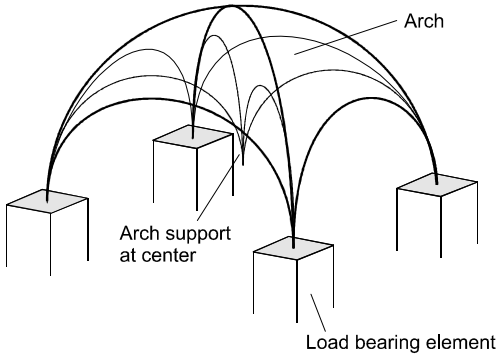

Fig. 16. Possible form of soil arching (triangular grid)

4 MODIFIED DESIGN APPROACH

The comparison of the soil pressure determined using the EBGEO and FEM in Fig. 18 shows enormous difference. Therefore, a modified approach has been developed based on the EBGEO (2008) design approach for the case of triangular pile arrangement. The modification is only on the determination of the vertical soil pressure on the surface of the geogrids in the areas between the piles.

The vertical soil pressure σ_{zo} on the surface of the geogrids between the pile-like elements can be calculated using Eq. 1 according to EBGEO (2008):

$$\sigma_{zo} = \lambda_1^{\chi} \cdot \left(\gamma_k + \frac{p_k}{h} \right) \cdot \left(h \cdot \left(\lambda_1 + h_g^2 \cdot \lambda_2 \right)^{-\chi} + \right.$$

$$\left. h_g \cdot \left(\left(\lambda_1 + \frac{h_g^2 \cdot \lambda_2}{4} \right)^{-\chi} - \left(\lambda_1 + h_g^2 \cdot \lambda_2 \right)^{-\chi} \right) \right) \qquad (1)$$

where

h_g arch height in m

$h_g = s/2$ for $h \geq s/2$

$h_g = h$ for $h < s/2$

h embankment height in m

γ_k soil unit weight in kN/m^3

φ_k angle of internal friction

p_k surcharge in kN/m^2

s spacing of the pile-like elements in m

$d = \sqrt{\frac{4 \cdot A_s}{\pi}}$ equivalent diameter of the pile like elements in m

A_s projected cross sectional area of the pile-like element at the level of the geogrids

$$\chi = \frac{d \cdot \left(\left(\tan^2 \left(45° + \varphi_k / 2 \right) \right) - 1 \right)}{\lambda_2 \cdot s}$$

$$\lambda_1 = \frac{1}{8} \cdot (s - d)^2$$

$$\lambda_2 = \frac{s^2 + 2 \cdot d \cdot s - d^2}{2 \cdot s^2}$$

According to EBGEO (2008), the pile spacing s is given by Eq. 2 (see also Fig. 17):

$$s = \max\{s_x, s_y\} \qquad (2)$$

The numerical analyses however show that there exists a base support for the arch at the middle of the geogrids, and hence a reduced spacing s given by Eq. 3 (see also Fig. 17):

$$s = s_L \qquad (3)$$

With reduced spacing according to Eq. 3 and using Eq. 1, the vertical soil pressure σ_{zo} can be determined and the EBGEO (2008) approach can be followed for remaining calculations.

A comparative presentation of the soil pressure and the maximum strain in geogrids is given in Fig. 18 and 19 respectively.

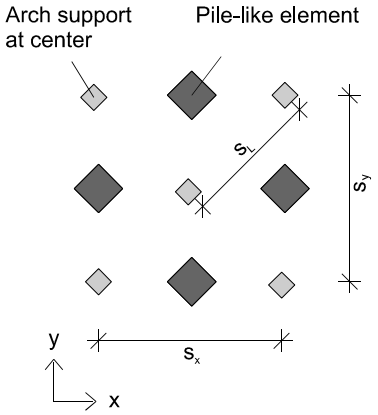

Fig. 17. Modified spacing for the design approach according to EBGEO (2008)

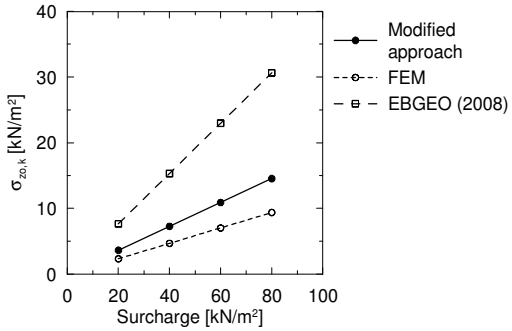

Fig. 18. Comparison of the soil pressure

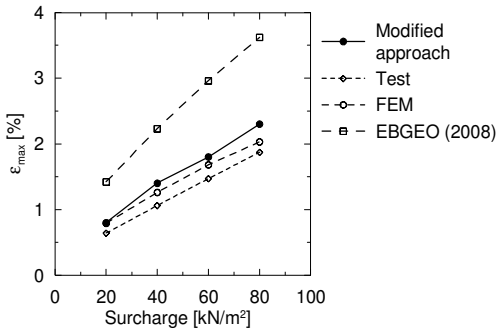

Fig. 19. Comparison of the maximum strain in geogrids

5 SUMMARY

Geosynthetic reinforced and pile supported embankments (GPE) is successfully used in the construction industry since beginning of the 1990. Essentially, the load transfer mechanism of the GPE system had been investigated for the case of rectangular and triangular pile arrangements.

In the case of the rectangular grid system, the soil arching model by Heitz (2006) has been verified. By triangular grid system however a different hyphothesis for the soil arching has been developed based the numerical analysis result, in which the arch can stabilize itself due to an additional base support at the middle. Based on this new finding, EBGEO (2008) design approach has been modified for the case of triangular grid system, so that an economical design of the geogrids is possible. The authors emphasize however that the modified approach shall be used with reservation, before it is verified by further study.

REFERENCES

EBGEO (2008). *Empfehlungen für Bewehrungen aus Geokunststoffen*. Deutsche Gesellschaft für Geotechnik e.V. (DGGT), in preparation

Heitz, C. (2006). Bodengewölbe unter ruhender und nichruhender Belastung bei Berücksichtigung von Bewehrungseinlagen aus Geogittern. *Schriftenreihe Geotechnik*, Universität Kassel, Issue 19

Kempfert, H.-G. & Stadel, M. (1995). Zum Tragverhalten geokunststoffbewehrter Erdbauwerke über pfahlähnlichen Traggliedern. *Geotechnik Sonderheft zur 4. Informations- und Vortragsveranstaltung über Kunststoffe in der Geotechnik der Deutschen Gesellschaft für Geotechnik e.V. (DGGT)*, München, 146-152.

Lüking, J. & Gebreselassie, B. & Kempfert, H.-G. (2008). Zum Lastabtrag von Geogittern in geokunststoffbewehrten Erdschichten über Pfahlelementen. *6. Kolloquium „Bauen in Boden und Fels“* der Technischen Akademie Esslingen, Ostfildern, 469-478

Zaeske, D. (2001). Zur Wirkungsweise von unbewehrten und bewehrten mineralischen Tragschichten über pfahlartigen Gründungselementen. *Schriftenreihe Geotechnik*, Universität Kassel, Issue 10

Zaeske, D. & Kempfert, H.-G. (2002). Berechnung und Wirkungsweise von unbewehrten und bewehrten mineralischen Tragschichten über punkt- und linienförmigen Traggliedern. *Bauingenieur* 77, 80-86